TURNTABLE-BASED AND ARTIFICIAL TEXTURE AIDED PHOTOGRAMMETRIC 3D RECONSTRUCTION AND SPECIFICATION MEASUREMENT OF SHUTTLECOCK

Sih-Han Wang [1] and Jen-Jer Jaw [2]
[1]National Taiwan University, Rm. 217, Civil Engineering, No. 1, Sec. 4, Roosevelt Rd., Da'an Dist., Taipei 106, Taiwan
Email: r10521808@ntu.edu.tw
[2]National Taiwan University, Rm. 208B, Civil Engineering, No. 1, Sec. 4, Roosevelt Rd., Da'an Dist., Taipei 106, Taiwan
Email: jejaw@ntu.edu.tw

KEY WORDS: photogrammetry, low-textured area, artificial texture, turntable, roundness

ABSTRACT: In the course of 3D object reconstruction, it is likely to experience incomplete reconstruction for those low-textured objects using photogrammetric means. Badminton is one of exciting sports, yet the 3D reconstruction of shuttlecock has never been easy due to its highly homogenous tone and symmetric shape, making it perfect to be our low-texture target. Under the low-cost consideration, a digital camera, projector, and turntable are used to capture images. By using the turntable and artificial tie points, the number of consumed projectors could be as less as one, and the full 360° coverage of image acquisition can be obtained. The artificial tie points arrange and join all partial point clouds into a complete set in Agisoft Photoscan platform, while the projected artificial textures support adequate richness of features for dense image matching. Besides, the scale control through precise distance measurements implements the 3D reconstruction task in a much easier and straightforward manner. The results of point cloud show that the completeness and geometrical accuracy of point clouds meet the required quality. However, the error of check scale in about 1.4 times of GSD, i.e. 0.14 mm suggests that further improvements are needed. Last but not least, 3D point clouds of shuttlecock made by the proposed method can provide efficiently and conveniently analytical data for specification measurement, such as roundness and lengths, and perform quality inspection for the process of shuttlecocks production.

1. INTRODUCTION

Close range photogrammetry has its advantages on 3D reconstruction of objects. However, due to the properties of the optical system, the stereo matching suffers from photometric distortions, specular surfaces, foreshortening, perspective distortions, repetitive patterns, transparent objects, occlusions, discontinuities and also uniform regions. Although there are corresponding methods tackling most of the problems above, photogrammetric 3D reconstruction still encounters a great challenge in the field of uniform or low-textured region. Low-textured regions are the scene with homogeneous patterns that easily lead to the failure of image matching. Putting artificial texture on the target can enrich the variety of textures. However, physical contact will hurt the target, especially inappropriate for the 3D reconstruction of cultural heritage. Exemplified study as shown in Figure 1 (Wenzel et al., 2013), even added with projected artificial textures (Menna et al., 2017; Nicolae et al., 2014), the location of target scene, operation condition, and hardware requirement, among others, still demand considerable concerns to arrange for an efficient and applicable work scheme, which is mainly aimed at this study.

In this study, we choose a shuttlecock as the low-textured target for performing 3D reconstruction, not only because the all in white feature of the shuttlecock, but also the production of it is a labor-intensive industry, requiring quality assessment through some specification measurements. Though some of the processes have been automated, for example, the insertion of feathers and the filling of the base glue, there still are lots of quality control process done by human eyes. Ai et al. (2011) employed region-dependent segmentation to automatically detect the tips of features and estimate the roundness of shuttlecock by 2D image processing techniques. On the other hand, 3D point clouds of shuttlecock, if provided, could also offer the specification measurement, such as length of the features and the roundness, up to 3D level.

Within the following sections, chapter 2 includes the methodology of our work scheme. Chapter 3 shows the process and 3D reconstruction results of shuttlecock, and the conclusions are given in Chapter 4.

(a) (b)

Figure 1. (a) photogrammetric acquisition of the white test object "Testy" using artificial texture from 3 video projectors. (b) result of orientations and sparse point cloud for 46 images. (Wenzel et al., 2013)

2. METHODOLOGY

2.1 Artificial Textures

Not all artificial textures can meet the standard of dense matching, the density and the entropy of textures should be both included in the design process. In this study, we use the artificial texture designed by Chen (2017), which followed the pseudo-random array proposed by MacWilliams and Sloane (1976). The size of the texture is 768*1024 pixels, and composed by four gray values (Figure 2). This texture is independent in each unit that meets the needs of randomness in different regions of texture.

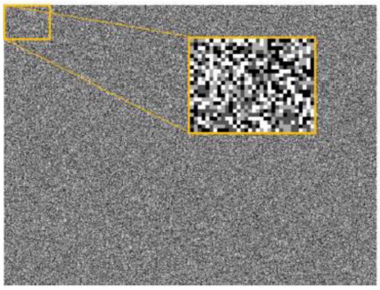

Figure 2. Artificial textures (Chen, 2017)

2.2 Equipment Arrangement and Image Acquisition

In this study, we utilize a projector, a digital camera combined with a turntable which can lower the number of projectors, and also decrease the requirement of image acquisition space (Figure 3(a)).

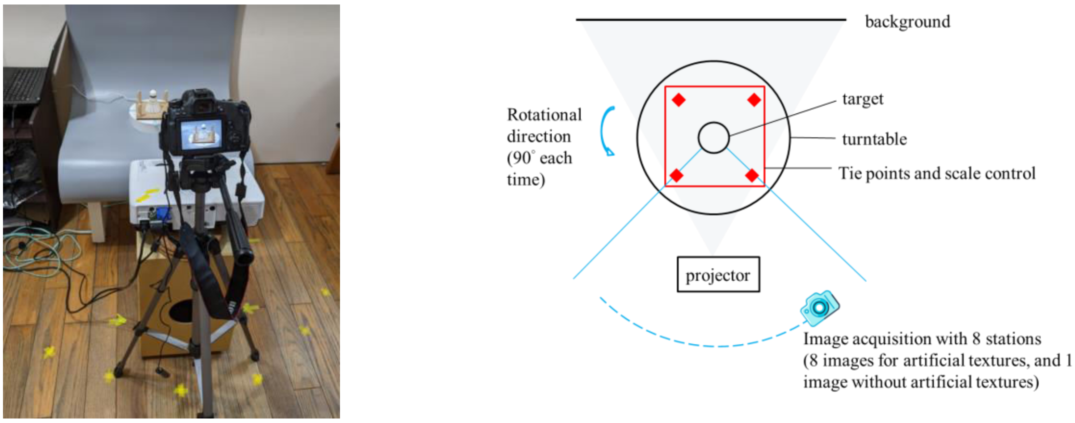

(a) real work scene : yellow marks on the floor are the locations where the camera is situated

(b) top view of work scene

Figure 3. Equipment arrangement and image acquisition

2.2.1 Projection Plans: To conduct an effective artificial texture projection, both the entropy of the image and the size of unit textures have to be determined. Once the unit texture is chosen, the size of unit texture in the object space would correspond to projection distance, shown as Figure 4. The longer the distance is, the bigger the size of texture is. According to the study of Chen (2017) "For dense matching, the size of the unit texture corresponding to the acquired image should not exceed 11.5 pixels", the relationship could be built as Eq. (1):

$$1 \leq \frac{X}{GSD} \leq 11.5 \tag{1}$$

Where X = the size of unit texture in object space (mm); GSD = ground sample distance (mm);
And R, throw ratio, is the ratio of projection distance and the width of screen, as shown in Figure 4. Then one can build the relationship between the distance of projection and the size of unit texture as Eq. (2):

$$X = \frac{D}{R * C_t} \tag{2}$$

Where D = distance between target and projector; C_t = number of unit texture along column.
To Substitute Eq. (2) into Eq. (1), and form Eq. (3) to decide a proper projection distance D.

$$C_p \leq D \leq 11.5 * C_p \tag{3}$$

Where $C_p = R * C_t * GSD$

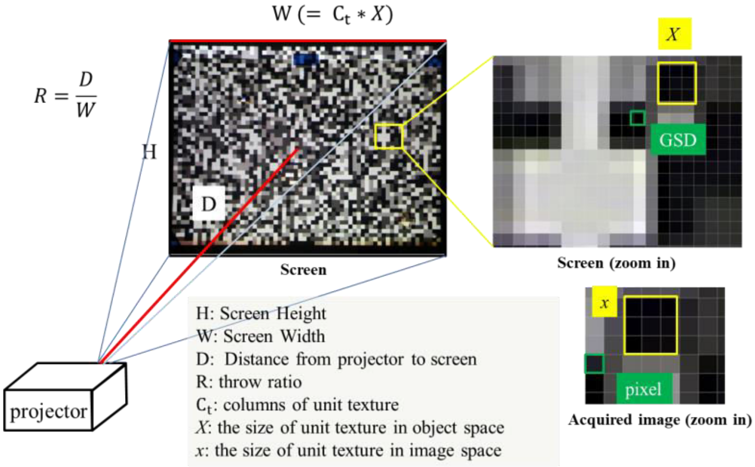

Figure 4. Illustration of unit texture

2.2.2 Settings: As afore-mentioned, the combination of a projector and turntable is proposed. Since one projector can only shed lights on half side of the target, rotating the target automatically by the turntable would complete projecting artificial texture and image acquisition. With this setting, we project artificial textures on one side with 8 images captured in a quarter of a circle and 1 image captured of the shuttlecock without artificial textures that would be further used in back-projection, and then rotate the turntable with 90 degrees to capture another quarter until accomplishing the whole circle, as illustrated in Figure 3(b).

2.3 Tie Points Design and Image Acquisition

With the projector fixed, the 360 degrees scene is partitioned into four quarters in the image acquisition process (Figure 5). 8 images could be acquired by setting the camera at 8 stations (as seen in Figure 3) and the complete image acquisition is made by rotating the turntable to stepwise bring scene of all four quarters to face the projector. Under such an image acquisition fashion and relatively monotone scene, it is not easy to find appropriate tie points for photo orientation. For this, we design four different colors of coded marks (Figure 7) attached on four faces of four columns, as shown in Figure 6. The coded marks, functioned as tie points, are arranged in a way that neighboring quarters are to be tied by using the same color marks, Point1~Point16 in Figure 6 for example, to simplify the identification and measurements. Note that one image with original texture of the shuttlecock in each quarter will be taken for the sake of retrieving real texture in the reconstruction stage.

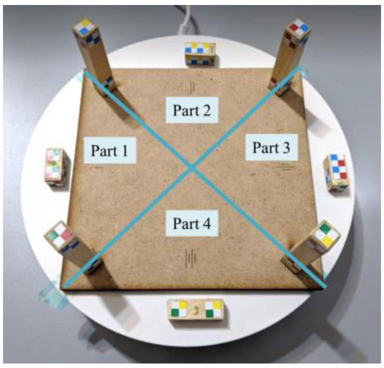

Figure 5. Scene partition

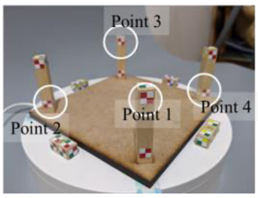

(a) red

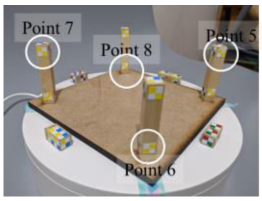

(b) yellow

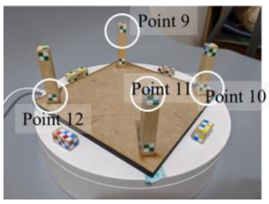

(c) green

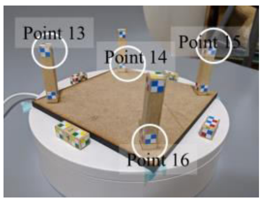

(d) blue

Figure 6. 16 tie points, 4 in each color, distributed equally on 4 columns

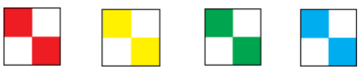

Figure 7. Four different colors of coded marks : Point 1~4 in red, point

5~8 in yellow, point 9~12 in green, and point 13~16 in blue

2.4 Scale Control

Aerial imagery, satellite imagery and other large-area recording methods of the ground surface by photogrammetric means have the need to fit the model system to the geodetic coordinate system. In order to convert the coordinate systems correctly, it is necessary to place ground control points (GCPs) in the survey area. The high quality and well distributed GCPs can not only provide the absolute spatial coordinate system, but also optimize the object-to-image correspondence. Conversely, when the errors of GCPs are too large or the distribution is poor, the positioning quality may not be satisfactory. For example, as shown in Figure 8, 3D reconstruction task of shuttlecock utilized GCPs to establish a spatial coordinate system and scale. Three GCPs were placed behind the shuttlecock, and the coordinates were measured manually with an iron ruler. As a result, the errors of coordinates may be as large as 1mm, leading to significant geometric deformation of 3D shuttlecock reconstruction as seen in the ellipse at cork base, and many apparent dislocations in the feather structure.

Figure 8. Shuttlecock reconstructed based on GCPs

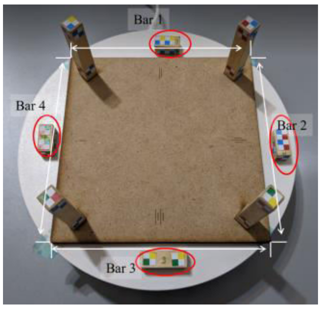

Figure 9. Four scale controls, each from corner to corner.

However, Small-scale 3D reconstruction tasks do not need to match with any spatial coordinate system, but rather focus on the accuracy of the model scale. To this end, this study sets up a scale control in all four parts, which is the distance from the corner to the next corner of the board (Figure 9), and also adds four check scales at four bars, all measured by using a digital caliper with about 0.03 mm measurement error.

2.5 Back Projection

After photo alignment and followed by dense image matching generating point clouds of shuttlecock projected with artificial textures, one can apply the collinearity equations with image point refinement, Eqs.(4) and (5), to back project the object coordinates of point clouds to the image without projecting artificial texture attaining the original texture and reconstructing the real 3D shuttlecock point clouds.

$$x_a - x_0 + \Delta x_{ref} = -f\frac{m_{11}(X_A - X_L) + m_{12}(Y_A - Y_L) + m_{13}(Z_A - Z_L)}{m_{31}(X_A - X_L) + m_{32}(Y_A - Y_L) + m_{33}(Z_A - Z_L)} \tag{4}$$

$$y_a - y_0 + \Delta y_{ref} = -f\frac{m_{21}(X_A - X_L) + m_{22}(Y_A - Y_L) + m_{23}(Z_A - Z_L)}{m_{31}(X_A - X_L) + m_{32}(Y_A - Y_L) + m_{33}(Z_A - Z_L)} \tag{5}$$

Where

(x_a, y_a): image point; (x_0, y_0): principal point; f: principal distance

(X_A, Y_A, Z_A): object point; $(X_L, Y_L, Z_L, \omega, \phi, \kappa)$: exterior orientation parameters

$m_{11} \sim m_{33}$: elements of rotation matrix

$\Delta x_{ref} = \bar{x}d^2K_1 + \bar{x}d^4K_2 + \bar{x}d^6K_3 + (2\bar{x}^2 + d^2)P_1 + 2P_2\overline{xy}$

$\Delta y_{ref} = \bar{y}d^2K_1 + \bar{y}d^4K_2 + \bar{y}d^6K_3 + 2P_1\overline{xy} + (2\bar{y}^2 + d^2)P_2$

$\bar{x} = x_a - x_0$; $\bar{y} = y_a - y_0$; $d^2 = \bar{x}^2 + \bar{y}^2$

K_1, K_2, K_3: coefficients of radial lens distortion ; P_1, P_2: coefficients of decentering lens distortion

2.6 Specification Measurement: Length and Roundness

With the point clouds of shuttlecock, one can measure the dimension and feature of interest in 3D space. The Badminton World Federation (BWF) sets the rules about the specification of the shuttlecock. For example, "The tips of the feathers shall lie on a circle with a diameter from 58 mm to 68 mm" and "The feathers shall have a uniform length between 62 mm to 70 mm when measured from the tip to the top of the base."

2.6.1 Point Cloud Filtering: To prevent the background points from interfering in the specification measurement of shuttlecock, a margin of RGB value is set to filter out most of the non-shuttlecock points, thus the tips of feathers can be easily found with the clear shape of a point intersected by two straight lines at each feather as illustrated in Figure 10. With the identification of tips of features, the lengths and the roundness of shuttlecock can be subsequently estimated.

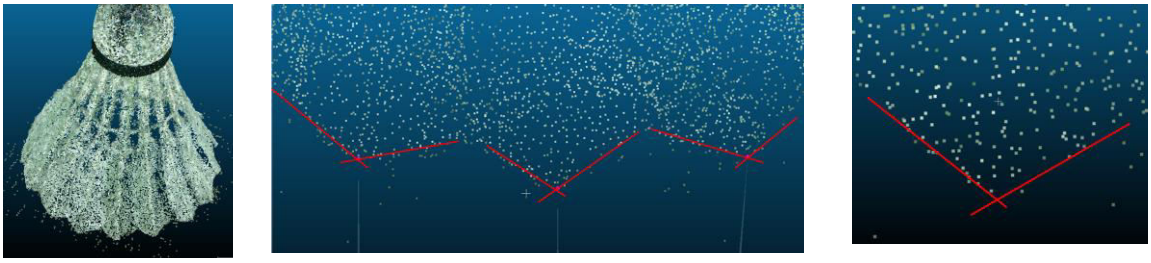

(a) shape of feathers (b) zoom into the tips of feathers

Figure 10. Point clouds of the feather of shuttlecock

2.6.2 Models of the Roundness: Although several definitions of roundness could be found in geometrical metric, the one calculating the difference between the maximum and minimum diameters offers the simplest estimation of roundness error. Note that the so-called diameters are to be determined by each candidate point to its farest point. On the other hand, circle fitting of 3D points of the feather tips would report the quality of radius and fitting errors. With the center of the fitted circle, the roundness error defined by the difference of maximum and minimum lengths from the center to the tips (Sui and Zhang) can be estimated. To realize such circle fitting, Gauss-Helmert model (Sphere fitting and plane fitting) with constraint (center of sphere situated on the plane), is employed to estimate the center of circle, radius, standard deviations of them and posterior a standard deviation of unit weight. Consequently, the roundness error can be also derived based on the estimated center of circle and the candidate tip points. Note that the roundness errors estimated by the above two methods, as shown in Figure 11, are not the same. The first one is based on the diameter while second one the center to the tips, thus the quantities between them are different.

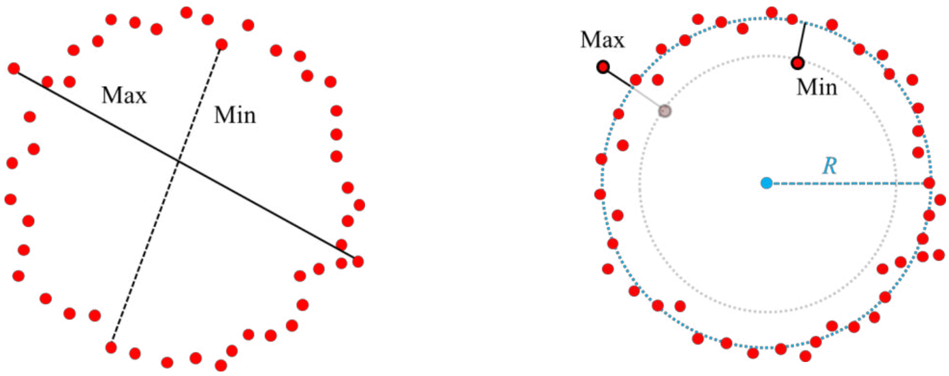

(a) method 1: the difference between the maximum and minimum diameters

(b) method 2: the difference between the maximum and minimum distances of the estimated center and the candidate points

Figure 11. Two methods of calculating the roundness error

3. EXPERIMENTS AND RESULTS

To verify the effectiveness of our proposed approach, the reconstruction of 3D point clouds of a shuttlecock is conducted through the following experiments with the employed instruments and the shuttlecock shown in Figure 12.

(a) Canon EOS 760D (b) Epson EB-1860 (c) turntable (d) digital caliper (e) shuttlecock

Figure 12. The instruments and the shuttlecock

3.1 Reconstruction without Artificial Textures

Owing to the low texture of scene, photo alignment for the image acquisition of shuttlecock with original texture leads to a failure (Figure 13) through the Agisoft Photoscan platform, not to mention point cloud generation.

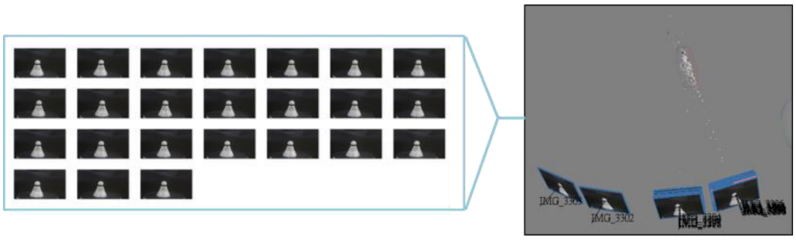

Figure 13. Failed reconstruction of shuttlecock

3.2 Reconstruction with Tie Points

Following the previous experiment but aided with tie points of designed coded marks, it succeeds in photo alignment and the generation of shuttlecock point cloud which shows some geometric deformations and holes in the cork base, as seen in Figure 14, largely contributed to the low texture on the shuttlecock itself resulting in poor performance in dense image matching both in Photoscan and SURE (Rothermel et al., 2012).

(a) image acquisition with coded marks

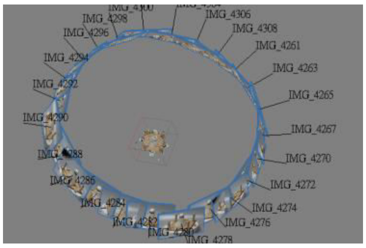

(b) results of orientation

(c) point clouds reconstructed via Photoscan

(d) point clouds reconstructed via SURE

Figure 14. Image acquisition with coded marks, results of orientation, and dense point clouds reconstructed via Photoscan and SURE

3.3 Reconstruction with Artificial Textures and Tie Points

With the failure and imperfection results in the previous experiments, it is clear that the tie points with easy identification and measurement and enhancement of texture on the shuttlecock have to be considered to support a quality reconstruction of shuttlecock point cloud. Thus, not only are tie points provided by coded marks but also artificial textures are projected by a projector onto the shuttlecock, as shown in Figure 15. The parameters of image acquisition and artificial texture are given in Table 1, and the acquired images are shown in Figure 16. The interior orientation parameters are pre-calibrated by Australis and exterior orientations are determined using Agisoft Photoscan platform. And it follows that SURE performs dense image matching to derive a dense point cloud with artificial texture. Finally, back-projecting the point cloud to retrieve the original texture of shuttlecock.

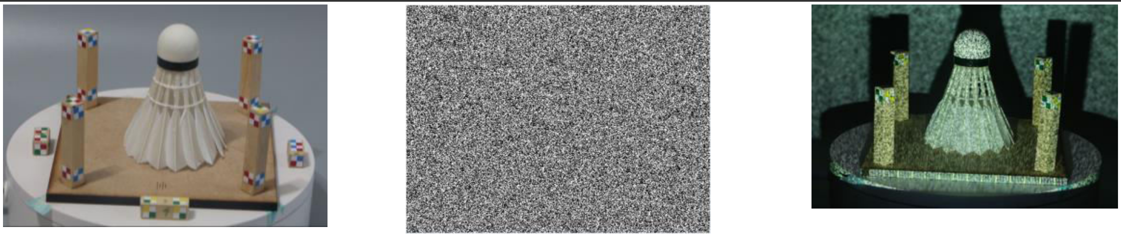

(a) targeted shuttlecock, corded marks and scalars on the turntable (b) artificial texture (c) targeted shuttlecock projected with artificial texture

Figure 15. Artificial textures and tie points added on the scene

Table 1. Image Acquisition parameters

Image size	1920*1280 pixels	Principal distance	85 mm
Pixel size	0.0117 mm	image baseline	195.2 mm
overlapping	80%	Object distance	1 m
GSD	0.1 mm	f-number	18
σ_Z	±0.03 mm	Size of unit texture in the object space	0.2 mm

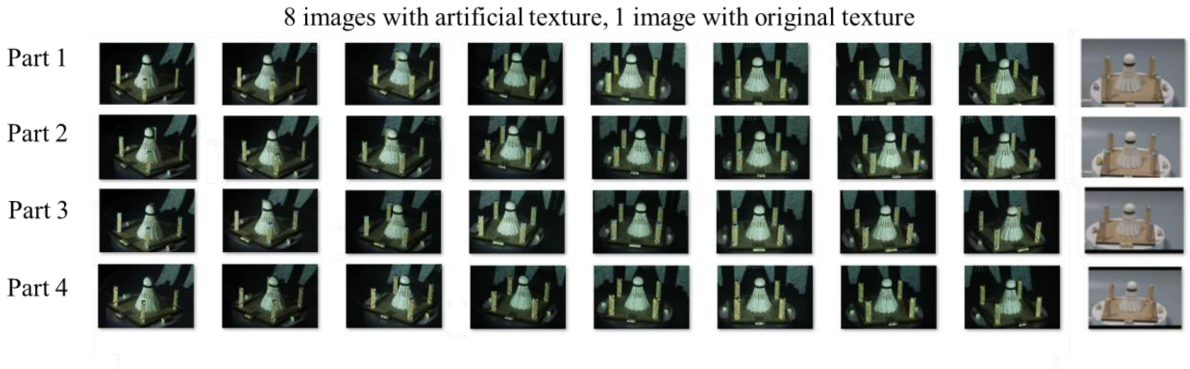

Figure 16. Image Acquisition

3.3.1 Analysis of 3D Dense Point Clouds: Figure 17 shows different views of point cloud results, including the whole shuttlecock, cork base, feathers and their branches. Table 2 shows the error and RMSE of check scales. The RMSE of check scales upon bundle block adjustment is about ±0.05 mm, less than 1 GSD (=0.1 mm), rendering the sub-pixel accuracy in image space. On the other hand, the RMSE of check scales in the dense point clouds reaches up to ±0.14 mm, about 1.4 times of GSD, the achievable accuracy when taking length measurement in the point clouds.

Table 2. Errors and RMSE of check scales

Check scales	Check 1	Check 2	Check 3	Check 4	RMSE
Errors through bundle block adjustment	0.07 mm	0.04 mm	-0.01 mm	0.05 mm	±0.05 mm
Errors of dense point cloud	0.09 mm	0.17 mm	0.07 mm	0.20 mm	±0.14 mm

Down on point cloud, first, there are no obvious deformations. The scale fits the real shuttlecock, also the density is high, except a little omission on the cork base due to low captured angle during image acquisition. Carefully look into cork base, the straight line and the arc of its shape are both correctly reconstructed. One can see clearly the contact point of cork base and the branch of feathers, and the detailed height differences do clearly show in the point cloud. Then turn the attention to the branches, it can be observed that some wrong matching points between branches exist, making the original hollow be filled up with point clouds. Finally, the satisfactory feather structure, with one tightly linked and nicely overlapped to another, validates the reconstruction of 3D shuttlecock by means of photogrammetric approach.

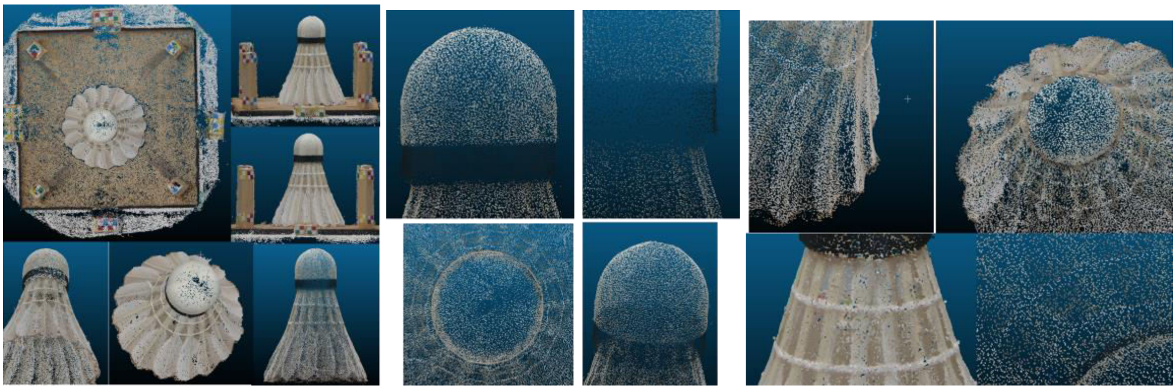

Figure 17. Results of dense point clouds reconstructed by SURE

3.3.2 Specification Measurement on Roundness: First, to clean the points of background out of the results. The margin of average RGB value is set at 100, values lower than this would be filtered out. Second, pick the tips. (Figure18). Third, calculate the roundness error and perform circle fitting for roundness as introduced in section 2.6.2. The result of roundness estimation can be seen in Table 3. Figure 19 illustrates how tips are fitted into a circle.

The roundness error estimated from directly calculating diameters is 1.16 mm ± 0.30 mm. And the circle fitting reports a radius of 33.50 mm ± 0.14 mm (equivalently a diameter of 67 mm) with the posterior a standard deviation of unit weight being about ±0.39 mm. And the roundness error based on the fitted circle is estimated to be about 0.87 mm ± 0.51 mm, which is 2.60% of the radius. Though currently there is no standard value of the roundness of shuttlecock, the 3D point cloud generated through the proposed approach does offer a convenient metric measurement for accessing the geometric specification of shuttlecock.

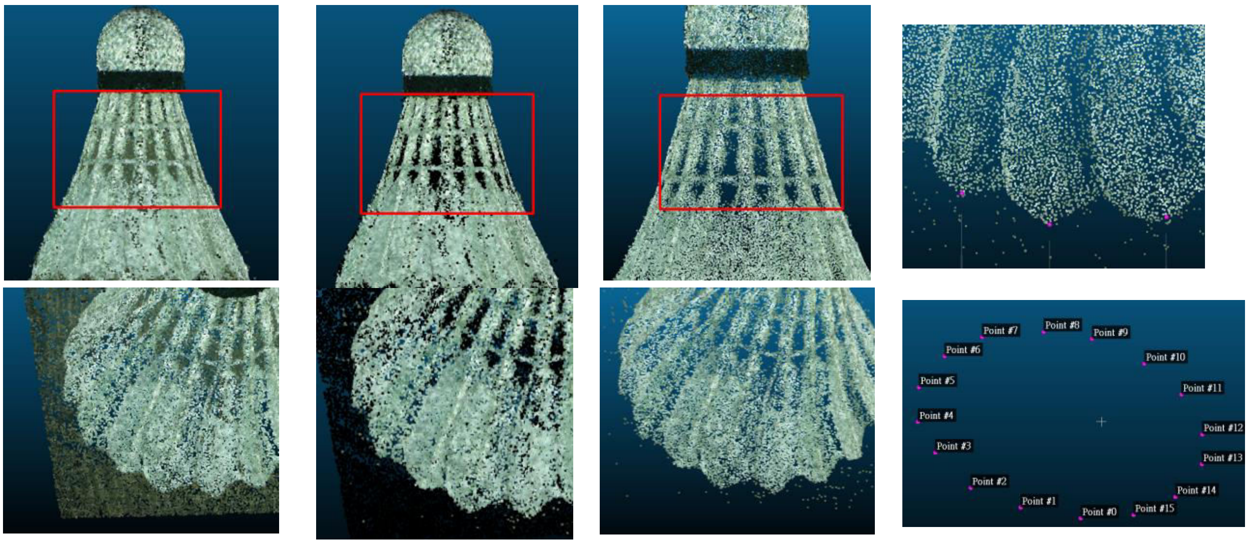

(a) original points (b) mark the background in black (c) clean the points (d) pick the 16 tips

Figure 18. The process of measurement

Table 3. Estimations of roundness

Model	Roundness error	Radius	Posterior standard deviation of unit weight
distance of Max.-Min.	1.16 mm ± 0.30 mm		
Circle fitting	0.87 mm ± 0.51 mm	33.50 mm ± 0.14 mm	± 0.39mm

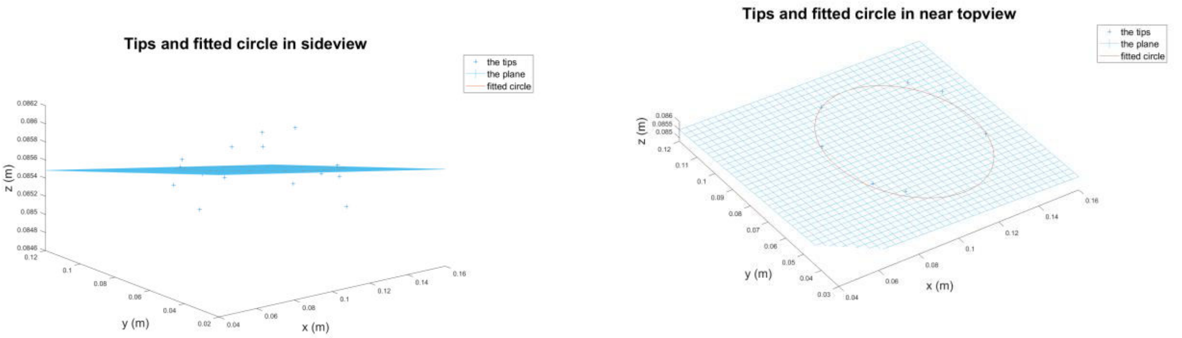

Figure 19. Circle fitting

3.3.3 Specification measurement on the Length of Feathers: Figure 20 shows the measured lengths in the point cloud. Table 4 gives the length measured, and the average is 61.94 mm ± 0.21 mm, a little shorter than the rule of BWF : "The feathers shall have a uniform length between 62mm to 70mm when measured from the tip to the top of the base."

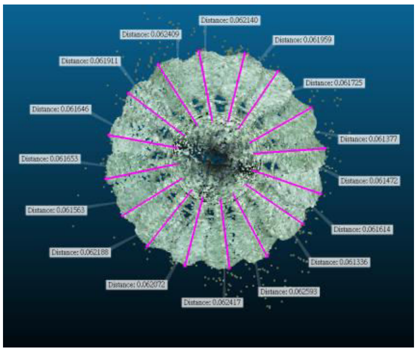

Figure 20. Length measurement

Table 4. Length of the feathers (unit: mm)

1	2	3	4	5	6	7	8
62.19	62.07	62.42	62.59	61.83	62.01	61.47	61.38
9	10	11	12	13	14	15	16
61.73	61.96	62.14	62.41	61.91	61.65	61.65	61.56
average			61.94 mm ± 0.21 mm				

4. CONCLUSIONS

Under the low cost condition, this research proposes an efficient and applicable work scheme by projecting artificial texture, arranging equipment combined with tie points and scale control to improve the accuracy of exterior orientation and dense image matching of low textured shuttlecock images. Geometrically, the reconstructed point clouds possess the quality of metric measurement up to 1.4 times GSD. Radiometrically, point clouds retrieve the original texture for presenting the real shuttlecock texture. The very same concept can be applied to other low textured objects.

On the other hand, the specification measurement of shuttlecock can be realized in 3D level, making the inspection, quality assessment, and other related applications of shuttlecock production and sport more appealing.

5. REFERENCES

Ai, X.F., Wang, R.H., Li, X.C., 2011. The Application of Roundness Error Measurement in the Detection of Badminton Appearance. Journal of Guangdong University of Technology, 28(4), pp.51-54. (in Chinese)

Chen, W.T., 2017. Using Artificial Texture to Assist 3D Reconstruction of Low Texture Imagery, Master Thesis, National Taiwan University. (in Chinese)

MacWilliams, F.J., Sloane, N., 1976. Pseudo-Random Sequences and Arrays, *In Proceedings of The IEEE*, 64(12), pp.1715-1729.

Menna, F., Nocerino, E., Morabito, D., Farella, E.M., Perini, M., Remondino, F., 2017. An open source low-cost automatic system for image-based 3D digitization. *The International Archives of the Photogrammetry, Remote Sensing and Spatial Information Sciences*, 62(2/W5), pp.155-162.

Nicolae, C., Nocerino, E., Menna, F., Remondini, F., 2014. Photogrammetry applied to problematic artefacts. *ISPRS*

Technical Commission V Symposium, pp. 23-25.

Rothermel, M., Wenzel, K., Fritsch, D., Haala, N., 2012. SURE: Photogrammetric surface reconstruction from imagery. *In Proceeding of LC3D Workshop.*

Sui, W., Zhang, D., 2012. Four Methods for Roundness Evaluation. *Physics Procedia*, 24, pp. 2159-2164.

Wenzel, K., Rothermel, M., Haala, N., Fritsch, D., 2013. Image acquisition and model selection for multi-view stereo, *International Archives of Photogrammetry and Remote Sensing, Remote Sensing and Spatial Information Sciences*, 40(5W), pp.251-258.